



The background image is an aerial view of a complex highway interchange with multiple lanes and overpasses. Several cars are visible on the roads. Overlaid on this image is a network diagram consisting of nodes (represented by small circles with a car icon) and edges (represented by dashed lines). The nodes are positioned at various points along the highway, suggesting a network of connected vehicles. The diagram illustrates the concept of wireless localization for connected vehicles.

# A Wireless Localization Algorithm With BPNN-MEA-QPSO for Connected Vehicle

**Lei Chen, Jiangfeng Wang, Zhijun Gao, Jiakuan Dong and Xuedong Yan**

*Are with the MOE Key Laboratory for Transportation Complex Systems Theory and Technology, Beijing Jiaotong University, Beijing, 100044, China. E-mail: 16114206@bjtu.edu.cn; wangjiangfeng@bjtu.edu.cn; 17114223@bjtu.edu.cn; 17120788@bjtu.edu.cn; xdyan@bjtu.edu.cn*

**Jian Wang**

*Is the corresponding author and is with department of automobile engineering, Beihang University, Beijing, 100044, China. E-mail: wj1974@buaa.edu.cn*

**Abstract**—As one of key technologies of connected vehicles (CVs) applications, wireless localization can provide accurate and reliable vehicle location for high occupancy tolling and safety critical vehicle applications, such as collision avoidance. Several artificial intelligence methods, such as back propagation neural network (BPNN) and particle swarm optimization (PSO) method, have been employed to optimize the pass-loss model and to improve the accuracy of wireless localization algorithm. However, in view of the stochasticity of initial weights and thresholds in BPNN, it is difficult to reach the global convergence. In this study, a novel double-layer architecture for wireless localization algorithm is proposed based on the optimization of initial weights and thresholds in BPNN and the refinement of search direction and step in PSO algorithm. Based on the architecture, the wireless localization algorithm integrating

Digital Object Identifier 10.1109/MITS.2019.2903433  
Date of publication: 18 March 2019

BPNN with mind evolutionary algorithm (MEA) and quantum-behaved PSO (QPSO) method is proposed and validated using the experiment data in field environment. The validation results show that the proposed localization algorithm has better localization accuracy by comparison with the other localization algorithms, which the average error of the proposed localization algorithm in field environment is about 19 meters. In addition, the localization accuracy shows an improving tendency with the increasing of the number of base stations connected to moving vehicle. The location error is less than 10 meters when the number of base stations connected to the moving vehicle is greater than 7. For the wireless localization in field environment, the accuracy is acceptable for CVs applications.

## I. Introduction

The popularity of vehicles provides great conveniences to people traveling. Meanwhile, many issues concerned arise accordingly with the sharp increasing of vehicles, such as traffic congestion, safety and environment pollution. In order to resolve these issues above-mentioned, various technologies related to connected vehicles (CVs) have sprung up, including dedicated short range communications (DSRC), swarm intelligence (SI), and artificial intelligence (AI) [1]–[5]. As a key component of numerous CVs applications, wireless localization can acquire the location of moving vehicles through the received signal strength received by moving vehicles from base stations and to improve the traveling efficiency and safety. However, the shortcomings of global positioning system (GPS), such as unavailability of GPS fixing and much lowered GPS positioning performance in terms of accuracy and reliability in a highly dense urban area due to GPS signal sheltered and interference, has been a motivation for recently emerging wireless localization algorithms based on vehicle-infrastructure communications. The traditional wireless localization algorithms include range-based algorithms, such as received signal strength Indicator (RSSI), and range-free algorithms, such as time of arrival (TOA), time difference of arrival (TDOA), angle of arrival (AOA). In view of the advantages of low cost, low power consumption, low communication overhead and low implementation complexity, the localization algorithm based on RSSI is applied widely [6]–[12]. In addition, the construction of roadside units (RSU) in smart city will provide a large number of base stations to enable wireless localization of moving vehicles.

For the localization algorithm based on RSSI, two steps are executed to complete the wireless localization of moving

vehicles. The first step is to calibrate the path-loss model to obtain distance between base stations and moving vehicles. Due to the received signal strength affected by various space environment factors, such as path loss and environment shadow fading, it is difficult to calibrate a precise path-loss model in field environment. The second step is to calculate the coordinates of moving vehicles using the calibrated path-loss model and the localization algorithms, such as least square (LS) method and multilateral localization algorithm. The positioning error between the calculating coordinate values and actual coordinate values of moving vehicles still exists in the optimization process.

Many scholars attempt to increase the localization accuracy through the optimization of the path-loss model. Yao and Han et al. proposed a novel distributed weighted search localization (WSL) algorithm by introducing a modified path-loss model based on RSSI. The WSL algorithm utilized the results of a centroid localization algorithm as the search initial point, and employed a new weighted search method to calculate the position of unknown nodes in a distributed and recursive manner [13]. Considering the feasibility of the path-loss model in the harsh environment, a new cooperative positioning method was proposed to improve the GPS estimates using internode range-rates based on the doppler shift of the carrier of DSRC signals. Depending on the speed of the participating vehicles and traffic intensity, improvement of up to 48% over the GPS accuracy was achieved [14]. To improve the GPS localization accuracy, Song and Li et al. also proposed a hybrid multi-sensor fusion strategy based on RSSI for vehicle localization, and this strategy achieved a good positioning performance in extended GPS-denied environments, such as tunnels [15]. Graefenstein and Bouzouraa studied the localization of a mobile robot using RSSI in low power. A novel algorithm was elaborated allowing for sub meter accuracy, and accounted for the noise and implicitly models the uncertainty [16]. In addition, other scholars adopted Kalman filter to reduce the accumulated errors of localization by separating the signal and noise [17], [18]. Zhang and Yang et al. presented a sequential fusion estimation method based on a novel square root cubature Kalman filter, which can help simplify the determination of the process noise covariance while maintaining a satisfactory estimation performance [19].

Besides the improvement of path-loss model, various artificial intelligence methods, including back propagation neural network (BPNN) and particle swarm optimization (PSO) algorithms, are introduced to optimize pass-loss model and to improve the accuracy of wireless localization algorithm [20]–[23]. The wireless localization of randomly deployed nodes in CVs was usually formulated as a multidimensional optimization problem. Li and Wen et al. proposed a distributed two-phase particle swarm optimization (PSO) algorithm to solve the flip ambiguity problem and to improve the

Based on the proposed two improvement strategies, a novel double-layer architecture of wireless localization algorithm, integrating BPNN with mind evolutionary algorithm (BPNN-MEA) and quantum-behaved PSO (QPSO) algorithm, is proposed to improve the wireless positioning accuracy in field environment.

each base station, mind evolutionary algorithm (MEA) is introduced to optimize the initial weights and thresholds in BPNN to ensure obtain the optimal value of the global convergence. Then, the concept of potential drop in quantum mechanics is introduced to control the search directions and step lengths of particles, which eliminates the randomness of search direction and step in PSO algorithm, overcomes the premature phenomenon, and acquires a more accurate localization of

efficiency and precision. Simulation results indicated that the proposed distributed localization algorithm was superior to the previous algorithms [24]. To solve dynamic vehicle routing problem, a new two-phase multi-swarm PSO approach was proposed and compared with previous single-swarm approach and with the PSO-based method. Several evaluation functions and problem encodings were proposed and experimentally verified on a set of standard benchmark data sets [25]. To avoid the problem of the fitness function being restricted to prediction of complex path when using genetic algorithm (GA), Anitha and Duraiswamy proposed a location prediction algorithm of moving vehicles by integrating PSO optimization algorithm and feed forward back propagation neural network (BPNN) [26]. Ni designed a fitness function according to the environment variable and proposes an improved node localization method of wireless sensor network based on PSO [27].

The current studies on wireless localization algorithms are mainly used in indoor environment [28], [29]. It is very difficult to acquire an accurate position of moving vehicle in field environment. The field environment is the environment which is a real outdoor environment where there are many real traffic participants. The procedure of wireless localization algorithm for moving vehicle in field environment mainly consists of two layers: ranging layer and positioning layer. Although several AI methods, such as BPNN and PSO, have been employed in those steps to acquire a more practical RSSI-distance relationship or to reach a higher computational accuracy of the coordinates of moving vehicles [30]–[33]. However, in ranging layer, in view of the stochasticity of initial weights and thresholds in BPNN, it is difficult to reach the global convergence. And in positioning layer, the randomness of search direction and step in PSO algorithm makes it hard to reach the optimal coordinate of moving vehicle when the distances between moving vehicle and those base stations are already known. In this study, two improvement strategies will be conducted in ranging layer and positioning layer to enhance the localization accuracy of moving vehicle in field environment. Firstly, considering the characteristic of space environment of

moving vehicle with lower computational cost. Based on the proposed two improvement strategies, a novel double-layer architecture of wireless localization algorithm, integrating BPNN with mind evolutionary algorithm (BPNN-MEA) and quantum-behaved PSO (QPSO) algorithm, is proposed to improve the wireless positioning accuracy in field environment. BPNN-MEA is used to establish ranging models in ranging layer based on the traveling state information of moving vehicle (e.g. location, velocity and heading angle) and RSSI values received by moving vehicles from base stations. Meanwhile, QPSO algorithm is adopted to reach a higher computational accuracy of the coordinates of moving vehicle in field environment. By improving the accuracies of both two layers, the proposed hybrid wireless localization algorithm, wireless localization algorithm integrating BPNN-MEA and QPSO (i-BMQ localization algorithm), can avoid the negative effects of low ranging accuracy and imprecise coordinate calculating procedure simultaneously, allowing i-BMQ localization algorithm to reach a higher positioning accuracy than the localization algorithms which only optimize one of the two layers in the wireless localization procedure or only adopt conventional methods to optimize the two layers. At last, the wireless localization algorithm integrating BPNN-MEA and QPSO (i-BMQ) is designed and validated using the experiment data in field environment.

## II. Methodology

### A. Architecture of i-BMQ Localization Algorithm

According to the two improvement strategies above-mentioned, the framework of the i-BMQ localization algorithm based on the double-layer architecture is shown in Fig. 1.

Based on the double-layer architecture, the proposed i-BMQ localization algorithm mainly consists of two layers.

**Ranging Layer:** Calibrating the path-loss model using BPNN-MEA and ranging measurement

Based on the signal feature analysis of RSSI data, the experiment data in field environment is refined using the K-means clustering algorithm. The calibrated path-loss model based on BPNN-MEA is described in detail. The distance



between moving vehicle and base stations is measured by the calibrated path-loss model.

**Positioning Layer:** Calculating the coordinates of moving vehicle using i-BMQ algorithm

The localization algorithm is designed in detail. The coordinates of moving vehicles is calculated using the ranging obtained by the calibrated path-loss model and the QPSO algorithm. At last, the proposed i-BMQ localization algorithm is validated using the testing data.

### B. Ranging Measurement

#### 1) Signal Feature Analysis of RSSI Data

To validate the performance of the proposed localization algorithm, in-field experiment data was collected from Microsoft campus in Redmond, WA [34]. Nine base stations were spread across five office buildings on the Microsoft campus, as illustrated in Fig. 2. The box in the Fig. 2, which covers an area of approximately  $500 \times 500\text{m}^2$ , bounds the region where at least one packet can be received by moving vehicles from any base station. Not all pairs of base stations were within wireless range of one another. Two moving vehicles provided a shuttle service around the campus about ten times a day, moving within a speed limit of about 40 km/h. The nine base stations and two vehicles had small desktops with Atheros 5213 chipset radios. The antennae were omnidirectional and are mounted on the roofs of the respective buildings and moving vehicles. The antennae employed by the nine base stations are large antennae, which can act as stable wireless signal sources for the experiment. Low-loss coaxial cables connect the radios (on top floors of the buildings) and antennae. The moving vehicles were equipped with an externally mounted GPS unit, GlobalSat's BU-353 GPS unit which is based on the SiRF Star III chipset, and outputs the traveling states information of moving vehicle (location, velocity, and heading angle) once per second. The uncertainty in the location estimate of this chipset is under three meters 95% of the time. The accuracy and frequency is high enough for the GPS data to serve as the ground truth.

All base stations were set to the same 802.11 channel for the experiments in this study. The moving vehicles received frames along with a hardware timestamp and PHY layer information such as RSSI in "monitor" mode.

When the moving vehicles travelled on the Campus every day, the signals was real-time received from different base stations. The experiment data consisted of the location, velocity, heading angle of moving vehicle and RSSI

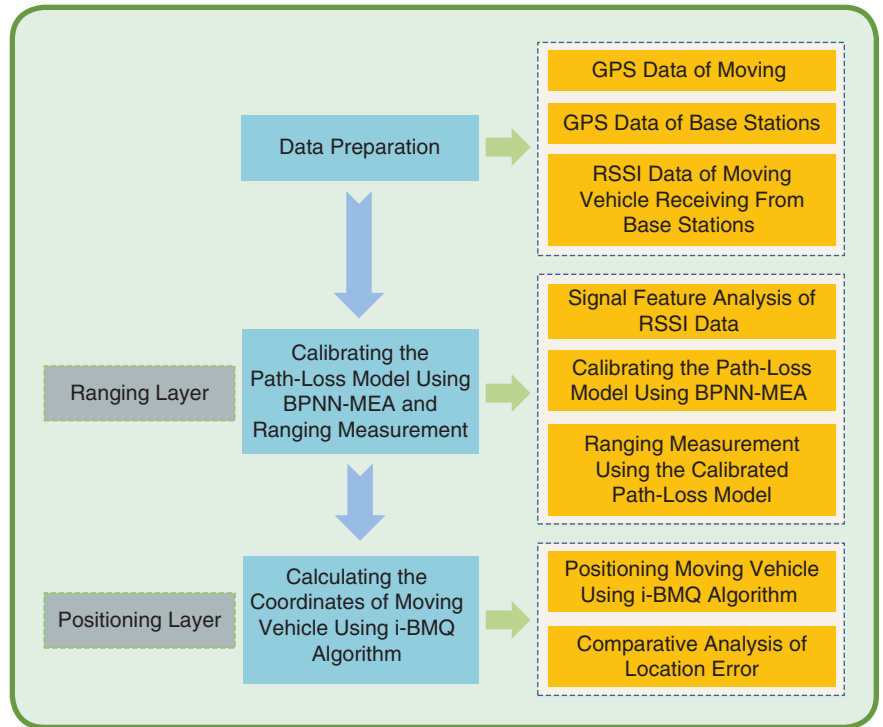


FIG 1 Architecture of i-BMQ localization algorithm.

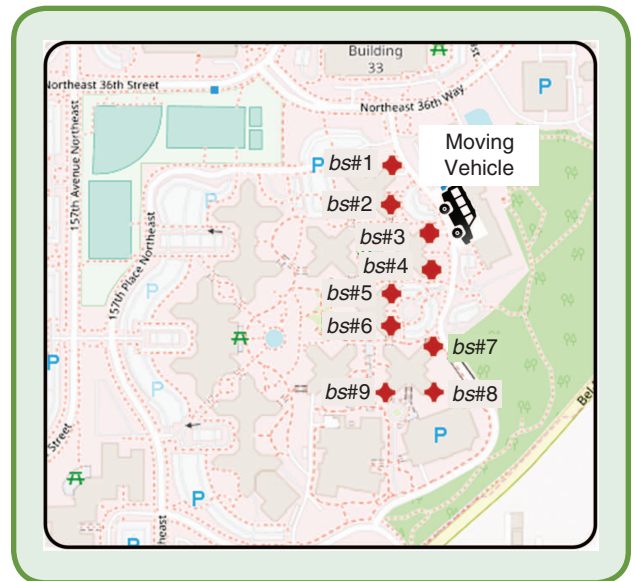


FIG 2 Layout of the nine base stations.

values received by moving vehicles from base stations. The experiment data was collected and marked by timestamp. Fig. 3 illustrates the collection process of in-field experiment data.

The experiment data of one moving vehicle in January 23, 2007 was selected as samples data to calibrate and validate the i-BMQ localization algorithm. The i-BMQ algorithm is

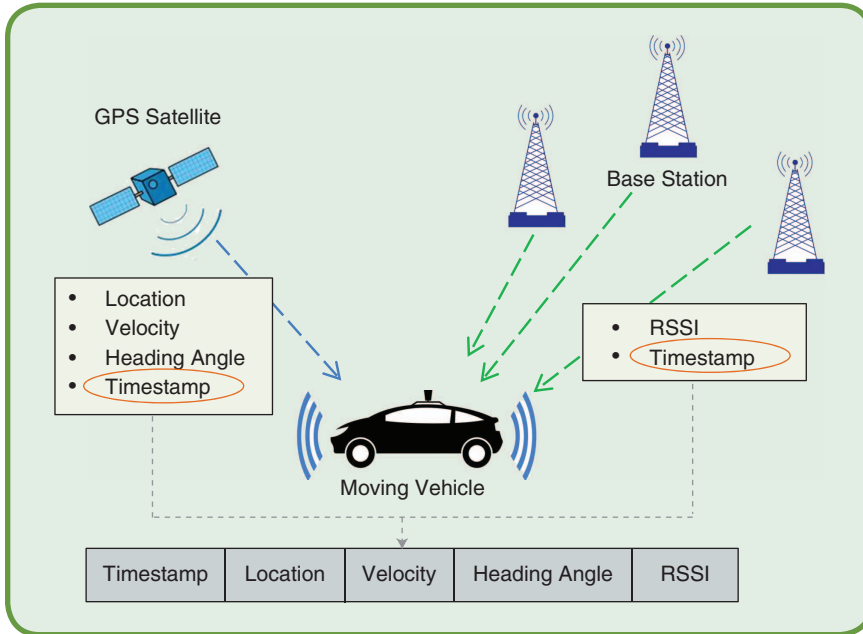


FIG 3 Collection process of in-field experiment data.

Table I. Sample instances of the in-field experiment data.

| Timestamp | Base station connecting moving vehicle | Longitude (W) | Latitude (N) | Speed (km/h) | Heading angle | RSSI (dBm) |
|-----------|--|---------------|--------------|--------------|---------------|------------|
| 15:24:48  | bs#1                                   | 122.1306      | 47.64245     | 14.94        | 48.22°        | 3          |
| 15:25:48  | bs#1                                   | 122.1306      | 47.64245     | 14.94        | 48.22°        | 4          |
| 15:26:35  | bs#2                                   | 122.1307      | 47.64257     | 17.24        | 182.64°       | 0          |
| 15:26:43  | bs#2                                   | 122.1307      | 47.64196     | 37.35        | 179.25°       | 1          |
| ...       | ...                                    | ...           | ...          | ...          | ...           | ...        |
| 15:46:48  | bs#3                                   | 122.1307      | 47.64196     | 37.37        | 179.25°       | 1          |
| ...       | ...                                    | ...           | ...          | ...          | ...           | ...        |

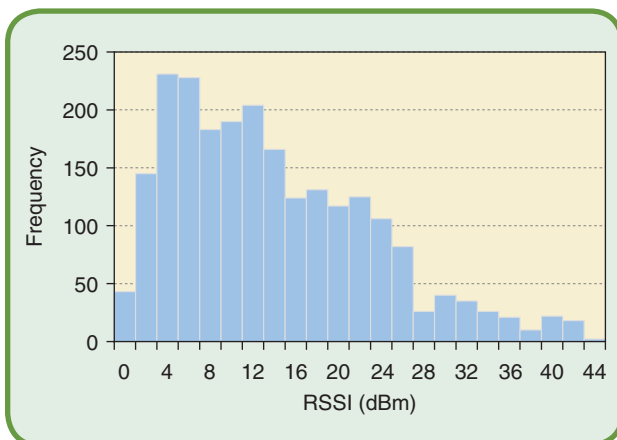


FIG 4 Distribution of RSSI values (from training samples data).

calibrated selecting the 15:00–15:30 in-field experiment data as training samples data, and is validated selecting the 15:30–16:00 in-field experiment data as testing samples data. The instances of samples data in-field experiment data were shown in Table I.

Because of wireless signals affected by space environment surround base stations (e.g. building, white background noise), the RSSI value received by the moving vehicle from base stations varies when the distance between the base station and moving vehicle changed. The range of RSSI values received by moving vehicle from the base stations is 0–44 dBm, and the frequency of the RSSI values is shown in Fig. 4.

As above mentioned, the spatial environment surrounding base stations has a large effect on the receiving RSSI values. Even when the moving vehicle are in the same location, the received RSSI values from each base station are also fluctuant, which is consistent with previous research [35], [36]. When keeping the moving vehicle stopping, the distribution of RSSI values received by moving vehicle from base station *bs#1* is shown in Fig. 5.

The stability of wireless signal has influence on the reliability of calibrated path-loss and ranging result based on RSSI. If the wireless signals of base stations in the study area are not stable enough, the fluctuating RSSI values received by moving vehicle at

the same position will make the whole study meaningless. To investigate whether the wireless signals of the nine base stations are stable enough to support the experiment and research, the study area is divided into 10000 (100\*100) sub areas equally by an invisible grid. Each sub area covers about 25 m<sup>2</sup> and the standard deviations of RSSI values received by moving vehicle during the day of experiment from each base station in each sub area are calculated separately (the sub areas with less than two received RSSI values, are considered as exceptions and ignored). Based on those standard deviations, a box-plot is plotted to analyze the discreteness of the nine wireless signals in the research area, as shown in Fig. 6.

As illustrated in Fig. 6, for each base station, in about three-quarters of the study area, the standard deviations of RSSI values received by moving vehicle are under 4 dBm

and in almost the whole study area, these standard deviations are under 8 dBm. Considering some factors like the existence of background interference such as white noise and the diversity of moving vehicle's traveling state, it can be concluded that the antennae are qualified enough for providing stable wireless signals over a long-term period.

In order to eliminate the influence of the space environment and explore the actual spatial distribution of RSSI values, colored points are used to mark the RSSI received from moving vehicle on map. For each sub area, the points are clustered into one point by using K-means clustering algorithm. To validate the effectiveness of K-means clustering algorithm, the scatter plot of RSSI values received by moving vehicle from the base station *bs#1* is shown in Fig. 7. The scatter plot can better reflect the distribution characteristics of RSSI values, which the farther distance corresponds to the larger RSSI values (i.e. the weaker signal strength). In addition, the simplification of redundant data also contributes to reduce the training time of the i-BMQ localization algorithm.

## 2) Calibrating the Path-Loss Model Using BPNN-MEA

The conventional path-loss models only consider the relationship between RSSI value and the distance from receiver to transmitter. However, by plotting RSSI distribution map for each base stations like Fig. 7, it is clear that those distributions are all not ideal concentric mode distribution, whose centers should be those base stations, the distributions of RSSI value were obviously affected by environment factors. However, those environment factors are mostly static, such as building and white background noise. Thus causing a fact that if the direction of the vector, which is formed by the

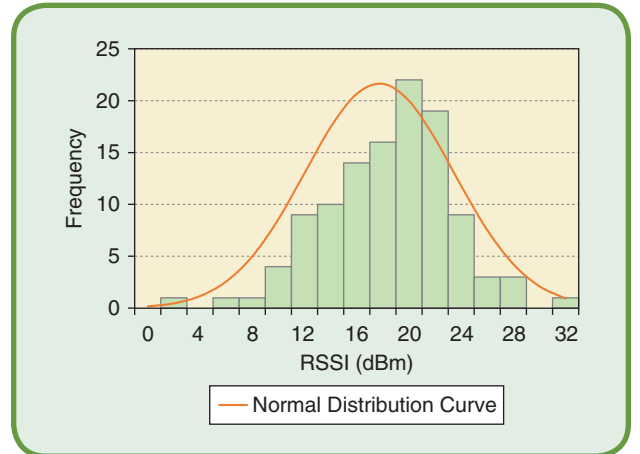


**FIG 5** Distribution of RSSI values received by moving vehicle from base station *bs#1* (from training samples data).

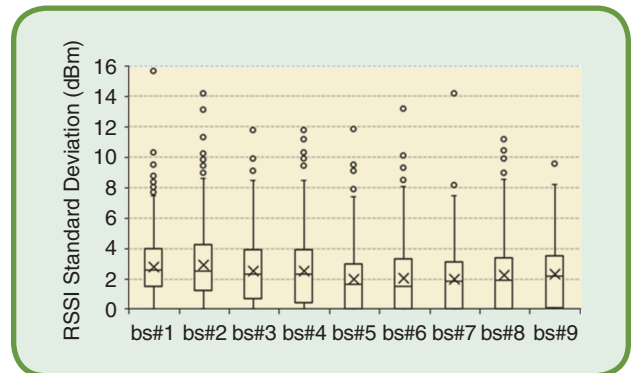


**FIG 6** Distribution of sub area RSSI standard deviation of the nine base stations (from the whole experiment data).

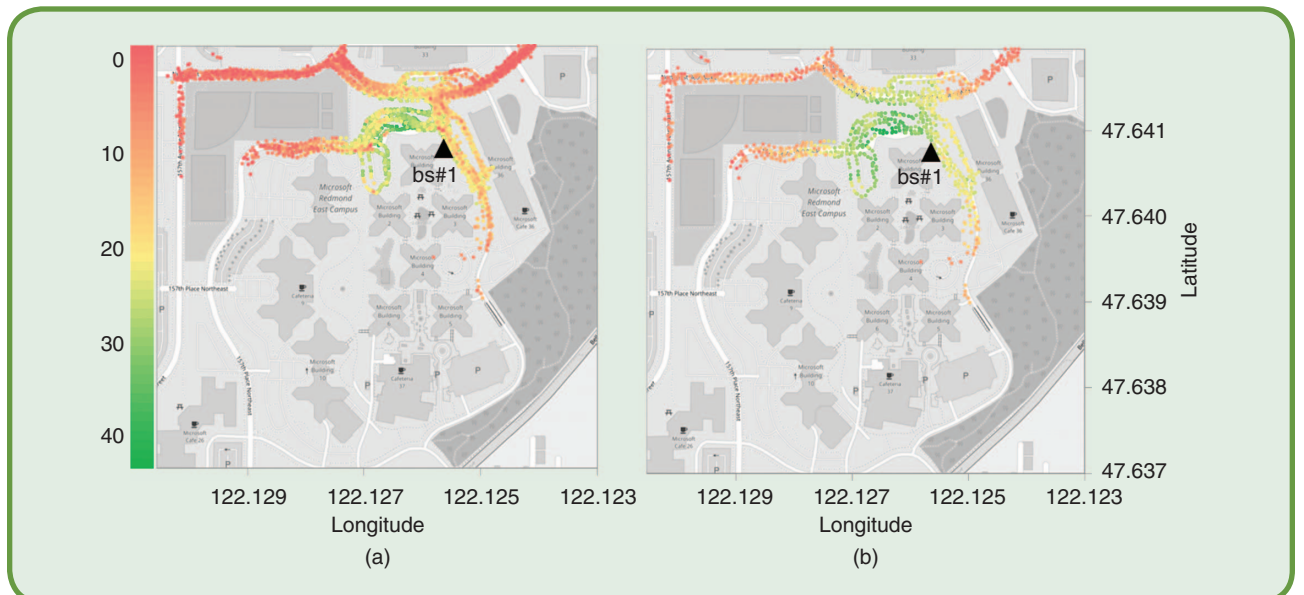


**FIG 7** Scatter plot of RSSI values received by the moving vehicle from the base station *bs#1* (from the whole experiment data). (a) Original data, (b) Clustered data.

To validate the performance of i-BMQ algorithm, the testing data is used to analyze the location accuracy. As a comparison, three localization algorithms, including multilateral localization with lognormal distribution model (ML-LDM), BPNN-QPSO and MEA-BPNN-PSO, are used to locate the moving vehicle using the same testing data.

one hidden layer structure is adopted, and the number of neurons ( $a$ ) in the hidden layer can be determined by the following empirical equation:

$$a = \sqrt{x_{\text{input}} + x_{\text{output}}} + \varepsilon \quad (1)$$

Where  $x_{\text{input}}$  and  $x_{\text{output}}$  are the number of input layer neurons and output layer neurons in BPNN respectively;  $\varepsilon$  is the empirical parameter, usually taking 1-10. In this study, the RSSI value received

location of base station and the location of moving vehicle, remains unchanged, the relationship between RSSI value and distance will be a one-to-one correspondence, which also remains unchanged. So, the relative position relationship between base station and moving vehicle can lessen the negative effects of environment factors. Based on RSSI distribution map, if there is a way, which could shrink the approximate scope where the moving vehicle might be, it is able to reduce the negative effects of environment factors as much as possible. In this study, the traveling state information of moving vehicle (e.g. previous known position, current velocity and current heading angle) can be utilized to realize this purpose. As a consequence, some conventional path-loss models are no longer applicable.

Several AI methods, such as BPNN, are suitable for establishing the relationship among the RSSI value, the traveling state information of moving vehicle and the distances from base stations to moving vehicle. However, in view of the stochasticity of initial weights in BPNN, it is difficult to reach the global convergence [30]–[33].

To solve this issue of initial weights, MEA is introduced to optimize the initial weights in BPNN in this study. MEA is an iterative learning method, which inherits the concepts of “population” and “evolution” in genetic algorithm (GA), and develops the processes of “convergence” and “dissimilation”. The convergence process can make the sub population reach its local optimization by analyzing the local environment, and the dissimilation process can find out the best sub populations and generate new sub populations to replace the others. By those two processes, MEA can optimize the initial weights in BPNN continually until reach the global convergence, and greatly reduces the prediction error caused by the random generation of hidden layer weights and thresholds.

The optimization process of initial weights in BPNN using MEA can be described as the following steps:

#### a) Structure of BPNN Determination

The structure of BPNN consists of the number of hidden layers and the number of neurons each layer. In this study,

from a certain base station, the longitude of the moving vehicle’s previous known position, the latitude of the moving vehicle’s previous known position, the current speed of the moving vehicle and the heading angle of the moving vehicle are considered as inputs for training, and the distances from moving vehicle to that certain base station is considered as output for training. So,  $x_{\text{input}}$  and  $x_{\text{output}}$  equal to 5 and 1 respectively, and  $\varepsilon$  is set to 2.55. Consequently,  $a$  equals to 5.

#### b) Initial Population Generation

When the structure of BPNN is determined, the total number ( $b$ ) of the initial weights and thresholds can be calculated:

$$b = (x_{\text{input}} + 1) * n + (n + 1) * x_{\text{output}} \quad (2)$$

A certain amount of individuals ( $m$ ) is randomly generated as initial population. Each individual  $j$  ( $j = 1, \dots, m$ ) includes all the initial weights and thresholds of the BPNN. The initial population is equally divided into several sub populations. Assuming each sub populations consisting of  $m$  individuals, the  $i$ th sub population  $S_i^{t,k}$  at the  $k$ th internal iteration in sub population of the  $t$ th global iteration can be described by:

$$\begin{aligned} S_i^{t,k} &= INV(N_{ij}^{t,k})_{j=1,\dots,m} \\ &= INV({}^0W_{ij}^{t,k}, {}^0V_{ij}^{t,k})_{j=1,\dots,m} \end{aligned} \quad (3)$$

Where  $INV()$  denotes transpose operator;  $N_{ij}^{t,k}$  denotes the information matrix of the  $j$ th individual in the  $i$ th sub population at the  $k$ th internal iteration in sub population  $S_i^{t,k}$  of the  $t$ th global iteration;  ${}^0W_{ij}^{t,k}$  denotes the initial weights between input layer and hidden layer of the  $j$ th individual in the  $i$ th sub population at the  $k$ th internal iteration in sub population  $S_i^{t,k}$  of the  $t$ th global iteration;  ${}^0V_{ij}^{t,k}$  denotes the initial weights between hidden layer and output layer of the  $j$ th individual in the  $i$ th sub population at the  $k$ th internal iteration in sub population  $S_i^{t,k}$  of the  $t$ th global iteration.



### c) Fitness Function of MEA

The fitness function of MEA is used to acquire the best initial sub populations. The back propagation process in BPNN is based on error between input layer and output layer. The transformed error can be used to characterize the performance of each individual and sub population. In this study, the reciprocal of mean square error is adopted as fitness function, which the higher value means the higher performance of the individual or sub population. For individual  $j$ , the fitness function  $\xi^{t,k}$  is as follows:

$$\xi^{t,k} = \frac{c}{\sum_{z=1}^c (Y_{NN}^{t,k} - Y_A^{t,k})^2} \quad (4)$$

Where  $c$  is the number of sample data in training sets;  $Y_{NN}^{t,k}$  is the distance obtained by trained BPNN at the  $k$ th internal iteration in sub population of the  $t$ th global iteration;  $Y_A^{t,k}$  is the actual distance output of the BPNN.

In order to optimal the population, the sub populations are first initialized. Using the fitness function, the individuals are listed in descending order in Global Billboard.  $M$  best individuals and  $T$  temporary individual are selected. Accordingly,  $M$  best sub populations and  $T$  temporary populations are generated around  $M$  best individuals and  $T$  temporary individuals. The amount of individual  $N$  in each sub population is:

$$N = \frac{m}{M+T} \quad (5)$$

The fitness value of sub population is stored in Local Billboard. The best individual of sub population  $S_i^{t,k}$  is defined as  $N_{i,best}^t$ .

### d) Convergence Operations

Convergence operations is an iterative process inside a sub population. This process makes all individuals move towards the best individual by obtaining the fitness value from local billboard.

All individuals in sub populations  $S_i^{t,k}$  follow normal distribution:

$$\bar{N}_i^{t,k}(\mu, \delta) \quad (6)$$

Where  $\mu$  is the central vector of the normal distribution, which is the position of the best individual  $N_{i,best}^t$  in sub population  $S_i^{t,k}$ , namely, the best initial weights in BPNN;  $\delta$  is the covariance matrix of the normal distribution. When all the individuals are independent,  $\delta$  is a diagonal matrix:

$$\delta = \text{diag}(\sigma_1^k, \sigma_2^k, \dots, \sigma_d^k, \dots, \sigma_b^k) \quad (7)$$

Where  $\sigma_d^k$  denotes the  $d$ th variable of diagonal matrix at the  $k$ th in internal iteration,  $d=1, \dots, b$ .

The original value of diagonal elements can be described as:

$$\sigma_d^0 = \frac{H_d - L_d}{10} \quad (8)$$

Where  $H_d$  and  $L_d$  denotes the upper limit and lower limit of weights and thresholds respectively.

In MEA, the mean of the normal distribution is the initial weights of best individual or temporary individual. The covariance of individuals in next iteration is:

$$\sigma_d^{k+1} = \gamma_1^k \sigma_d^k + \gamma_2^k \lambda_d^k \quad (9)$$

Where  $\gamma_1^k, \gamma_2^k$  are random seeds distributed uniformly on  $[0.1, 0.5]$ ;  $\lambda_d^k$  is the distance between best individuals of iteration  $k$  and  $k-1$ .

When the internal iteration reaches superior limit, or the position of the best individual  $N_{i,best}^t$  doesn't change in consecutive several iterations, the internal iteration stops and the fitness value  $\xi^{t,k}$  of the best individual  $N_{i,best}^t$  is the score of the sub population  $S_i^{t,k}$ .

### e) Dissimilation Operations

In this process, the new sub populations are formed by redistributing the individuals of the replaced and abandoned sub populations to assure that the number of sub populations remains constant. Then the new sub populations also participate in global competition with the best sub populations.

### f) Optimal BPNN Acquisition

When the global iteration reaches superior limit 1000 or the score of the best sub population doesn't change in consecutive 3 iterations, the global iteration stops. The sub population with the highest score is the global best subpopulation  $N_{g,best}$ , and the according best individual is the optimal initial weights and thresholds of the BPNN. The trained BPNN with the optimal initial weights and thresholds is the path-loss model calibrated by BPNN-MEA.

It is noteworthy that the signal of different base station has different RSSI distribution features. Low ranging accuracy will be caused using the same calibrated path-loss model to estimate the distances between moving vehicle and different base stations. Therefore, it is necessary to calibrate path-loss models individually for each base station.

The calibration process of the path-loss model using BPNN-MEA is shown in Fig. 8.

In Fig. 8,  $t$  stands for  $t$ th step of global iteration;  $k$  stands for  $k$ th step of internal iteration in sub population;  $N_{ij}^{t,k}$  stands for the  $j$ th individual in the  $i$ th sub population at the  $t$ th step of global iteration and the  $k$ th step of internal iteration in sub population  $S_i$ , each individual represents a BPNN with different initial weights between input layer and hidden layer ( ${}^0W_{ij}^{t,k}$ ) and different initial weights between



hidden layer and output layer ( ${}^0V_{i,j}^{t,k}$ ); the inputs of BPNN is  $X = (X_1, X_2, X_3, X_4, X_5)$ ,  $X$  includes the RSSI and the traveling state of the moving vehicle,  $X_1$  stands for the RSSI value received from a certain base station,  $X_2$  stands for the longitude of the moving vehicle's previous known position,  $X_3$  stands for the latitude of the moving vehicle's previous known position,  $X_4$  stands for the current speed of the moving vehicle,  $X_5$  stands for the heading angle of the moving vehicle; the output of BPNN is  $Y$ , which includes the distances between moving vehicle and a certain base station; the training data used for calibrating the model are randomly divided into two parts, one part contains the 70% of the data, serving as the training set, the other part contains the rest of the data, serving as the testing set;  $\xi_{i,k}^{t,k}$  is the fitness function value of individual  $N_{i,j}^{t,k}$ ;  $N_{i,pbest}^t$  is the best individual of sub population  $S_i$  at  $t$ th step of global iteration;  $N_{gbest}^t$  is the global best individual when the iteration is over. Individual  $N_{i,j}^{t,k}$  has a position described by  $N_{i,j}^{t,k} = ({}^0W_{i,j}^{t,k}, {}^0V_{i,j}^{t,k})$ , namely, the initial weights for BPNN of this individual.

### 3) Ranging Measurement Using the Calibrated Path-Loss Model

When the moving vehicle travels in the research area, at a certain moment, it can receive one or more RSSI values from in-field base stations simultaneously. Assuming that the number of base station signals received by moving vehicle at a certain moment is  $P$  ( $P$  varies from 1 to 9). Taking the received RSSI value of  $P$  base stations and the previous known location, current velocity and current heading angle of moving vehicle as input matrix, the distances between moving vehicle and each base stations  $e$  ( $e=1, \dots, P$ ) are obtained using the calibrated path-loss model for each base stations.

### C. Calculating the Coordinates of Moving Vehicle Using i-BMQ Algorithm

When  $P$  is greater or equal to 3, which means at least 3 estimated distances between moving vehicle and  $P$  base sta-

tions are available, it is possible to obtain the coordinate of moving vehicle if the coordinates of those base stations are known. Assuming  $(x, y)$  is the possible coordinate of moving vehicle and  $(x_e, y_e)$  is the coordinate of base station  $e$ . The location of moving vehicle is essentially an optimization problem and the optimal solution  $(x^*, y^*)$  is searched to minimize the objective function. The objective function is as follows.

$$\min f(x, y) = \frac{1}{P} \sum_{e=1}^P (\sqrt{(x-x_e)^2 + (y-y_e)^2} - \hat{d}_e)^2$$

$$\text{s.t. } \begin{cases} x > 0 \\ y > 0 \end{cases} \quad (10)$$

Where  $\hat{d}_e$  denotes the distance between moving node and the base station  $e$ .

PSO is feasible for optimizing the objective function because of its quick convergence and moderate demand for computing resources, which can be used to calculate the coordinates of moving vehicle in field environment. In the solution space, the position  $(x_z, y_z)$  of particle  $z$  of particle swarm represents a possible coordinate of moving vehicle, but may not be the optimal solution of the objective function. When the optimal value of the objective function is obtained, the highest location accuracy is acquired accordingly.

The optimal value of the objective function is discovered through the movements of particle of particle swarm. Considering the limitation of maximum convergence speed during the searching process, the searching area is limited in each iteration and the PSO algorithm is unable to reach the global optimization all the time. To avoid this issue, the quantum-behaved particle swarm optimization algorithm (QPSO) is introduced in this study, and the concept of potential drop is also introduced to attract the particles in QPSO to reach the global optimization.

When the particles are in the potential field of the position, the particle state is depicted by wave function  $\phi(\cdot)$ .

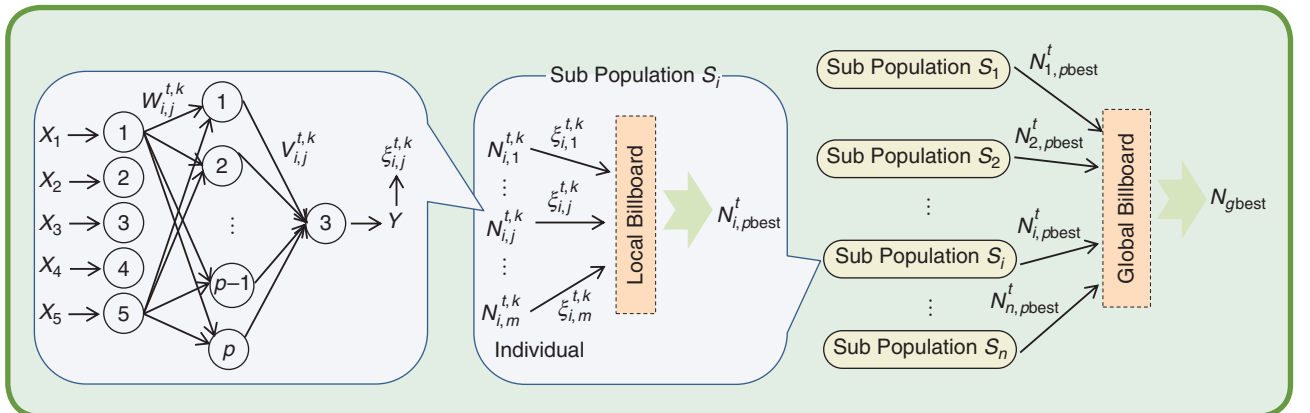


FIG 8 Calibration process of the path-loss model using BPNN-MEA.

In two dimensional spaces, assuming that there is an attraction potential field for a particle, the wave function of each dimension is:

$$\phi[x_{i,j(t+1)}] = \frac{1}{\sqrt{L_{i,j(t)}}} \exp\left[-\frac{|x_{i,j(t+1)} - \lambda_{i,j(t)}|}{L_{i,j(t)}}\right] \quad (11)$$

$$\lambda_{i,j(t)} = \varphi pbest_{i,j(t)} + (1 - \varphi) gbest_{j(t)} \quad (12)$$

Where  $x_{i,j(t+1)}$  is the position of particle  $i$  in the  $j$ th dimension at the  $(t+1)$ th iteration;  $L_{i,j(t)}$  is the characteristic length of particle  $i$  affected by the potential field of attraction  $i$  in the  $j$ th dimension at the  $t$ th iteration;  $\lambda_{i,j(t)}$  is the position of attraction  $i$  in the  $j$ th dimension at the  $t$ th iteration;  $pbest_{i,j(t)}$  is the  $j$ th dimension of the best position discovered by the particle  $i$  at the  $t$ th iteration;  $gbest_{j(t)}$  is the  $j$ th dimension of the global best position discovered by all particles at the  $t$ th iteration;  $\varphi$  is random number between 0 and 1.

The position of the particle  $i$  can be obtained through the following equation:

$$x_{i,j(t+1)} = \lambda_{i,j(t)} \pm \frac{L_{i,j(t)}}{2} \ln\left[\frac{1}{u_{i,j(t)}}\right] \quad (13)$$

Where  $u_{i,j(t)}$  is random number between 0 and 1.

The mean best position  $mbest$  is:

$$mbest_i(t) = \frac{1}{M} \sum_{i=1}^M pbest_i(t) = \left( \frac{1}{M} \sum_{i=1}^M pbest_{i,1(t)}, \frac{1}{M} \sum_{i=1}^M pbest_{i,2(t)}, \dots, \frac{1}{M} \sum_{i=1}^M pbest_{i,N(t)} \right) \quad (14)$$

So, the characteristic length  $L_{i,j(t)}$  is:

$$L_{i,j(t)} = 2\alpha |mbest_{j(t)} - x_{i,j(t)}| \quad (15)$$

The iterative equation of the particle's position is:

$$x_{i,j(t+1)} = \lambda_{i,j(t)} - \alpha |mbest_{j(t)} - x_{i,j(t)}| \times \ln\left[\frac{1}{u_{i,j(t)}}\right] \text{ if } k \geq 0.5 \quad (16)$$

$$x_{i,j(t+1)} = \lambda_{i,j(t)} + \alpha |mbest_{j(t)} - x_{i,j(t)}| \times \ln\left[\frac{1}{u_{i,j(t)}}\right] \text{ if } k < 0.5 \quad (17)$$

$$\alpha = (1 - \alpha_{\text{beta}}) \times \frac{t_n - t}{t_n} + \alpha_{\text{beta}} \quad (18)$$

Where  $k$  is random number between 0 and 1;  $t_n$  is the maximum number of iteration;  $\alpha$  is contraction-expansion coefficient;  $\alpha_{\text{beta}}$  is the initial contraction-expansion coefficient, which is the only specific parameter in QPSO algorithm, and can control the convergence speed of the algorithm.

When reaching the convergence criteria, the global best position  $(x^*, y^*)$  is the optimal solution of the objective

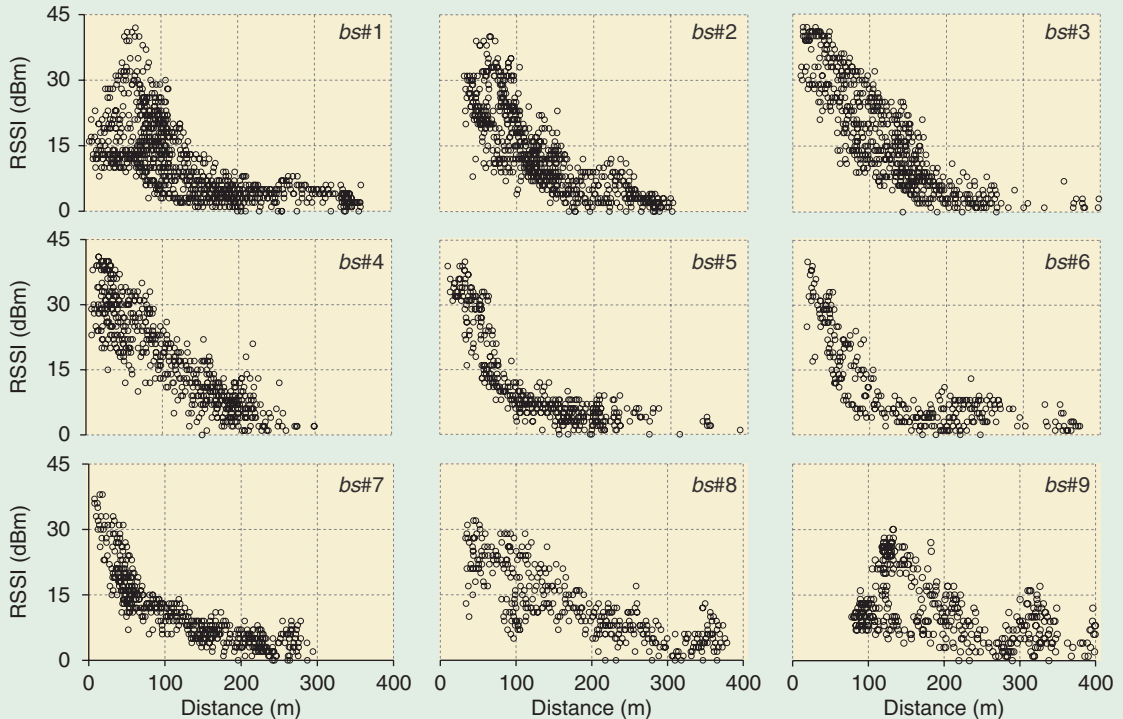


FIG 9 RSSI values vs. distance distributions of each base station.

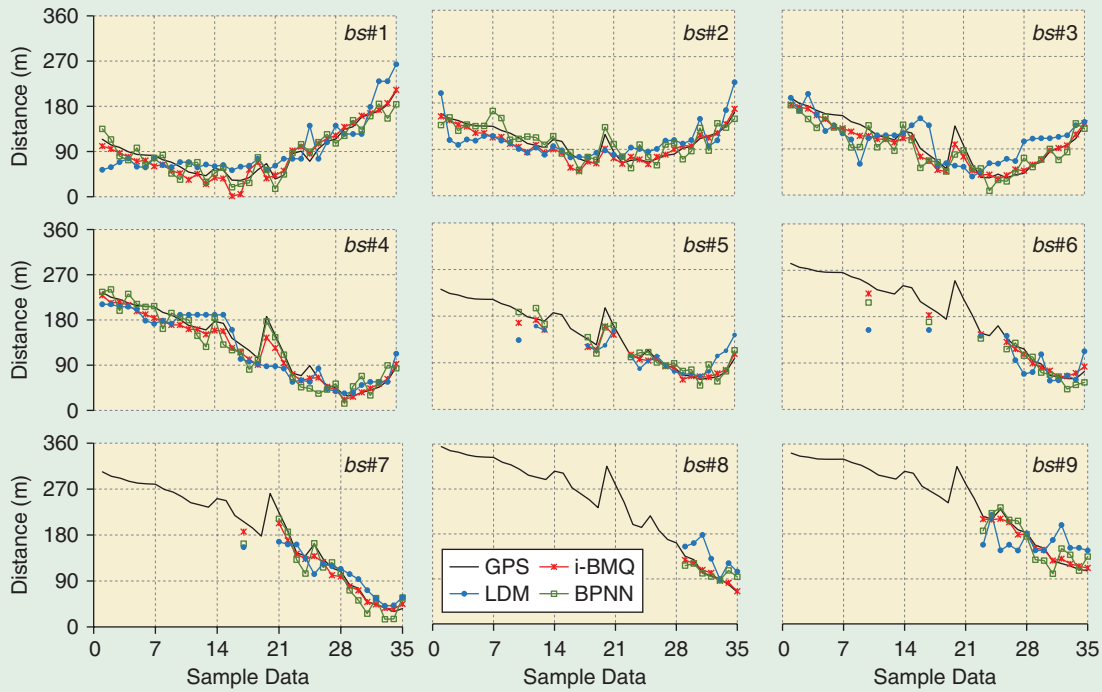


FIG 10 Ranging results.

function, and is the calculated coordinate of moving vehicle using i-BMQ algorithm.

### III. Simulation and Results

To validate the performance of i-BMQ algorithm, the testing data is used to analyze the location accuracy. As a comparison, three localization algorithms, including multilateral localization with lognormal distribution model (ML-LDM), BPNN-QPSO and MEA-BPNN-PSO, are used to locate the moving vehicle using the same testing data. The principle of ML-LDM refers to reference [37] and the principle of BPNN-QPSO and MEA-BPNN-PSO refers to the methodology in this study.

#### A. Analysis of Ranging Measurement

In this study, the 15:30–16:00 in-field experiment data in January 23, 2007 is selected as the original testing data. The original testing data is refined using K-means clustering algorithm to obtain the final testing data. The path-loss model is calibrated with the final testing data using the proposed BPNN-MEA. Considering the different space characteristics of each base station, the path-loss model for nine base stations are plotted, as shown in Fig. 9.

As illustrated in Fig. 9, the relationship between distance and RSSI each base stations generally shows the logarithm distribution. However, there is a certain difference among those distributions. By comparison, the scatter diagrams of base station *bs#8* and *bs#9* have a poor fitting for logarithm

distribution. The reason is probably caused by the larger distance between the base stations and the moving vehicle. The larger distance between the base stations and the moving vehicle implies the greater signal attenuation, thus making the RSSI received by moving vehicle have a bigger stochastic fluctuation. Finally, the relationship between distance and RSSI has a poor fitting for logarithm distribution.

Using the calibrated path-loss model, the distances between the moving vehicle and the base stations are obtained through the receiving RSSI. The ranging results are shown in Fig. 10.

As shown in Fig. 10, because of the limitation of transmitting power, the interference of the obstacles and the orientation of the antennas, the moving vehicle always lost connection with base stations when travelling. Generally, the ranging result using i-BMQ localization algorithm is better than the other methods.

By comparison, the traditional lognormal distribution model (LDM) and BPNN is also selected to measure the distance. The mean absolute error (MAE) and mean squared error (MSE) of three ranging results are shown in Table II.

As shown in Table II, for each base station, both MAE and MSE of the proposed i-BMQ localization algorithm are lower than the other methods. The i-BMQ localization algorithm shows a better ranging performance.

#### B. Analysis of Localization Accuracy

In the ranging layer, the distances between the moving vehicle and the base stations are real time obtained. Based on



Table II. MAE (M) and MSE of the ranging results.

| No. base stations | i-BMQ |        | BPNN  |        | LDM   |         |
|-------------------|-------|--------|-------|--------|-------|---------|
|                   | MAE   | MSE    | MAE   | MSE    | MAE   | MSE     |
| bs#1              | 11.63 | 193.54 | 14.61 | 263.56 | 24.07 | 861.17  |
| bs#2              | 9.66  | 160.79 | 13.84 | 264.87 | 21.83 | 628.34  |
| bs#3              | 10.53 | 174.37 | 18.06 | 515.21 | 27.34 | 1168.39 |
| bs#4              | 11.68 | 215.00 | 15.77 | 412.61 | 20.69 | 735.80  |
| bs#5              | 9.30  | 170.09 | 10.08 | 189.90 | 20.10 | 793.06  |
| bs#6              | 8.16  | 89.11  | 15.06 | 325.66 | 24.91 | 1205.43 |
| bs#7              | 9.08  | 140.80 | 16.71 | 399.49 | 21.34 | 772.76  |
| bs#8              | 5.04  | 29.30  | 12.88 | 308.29 | 35.18 | 1692.98 |
| bs#9              | 5.73  | 55.70  | 18.04 | 434.29 | 37.67 | 2043.08 |

Table III. Parameters settings of QPSO AND PSO.

|      | Parameter                                 | Value |
|------|---|-------|
| QPSO | populations                               | 25    |
|      | iterations                                | 100   |
|      | initial contraction-expansion coefficient | 0.5   |
| PSO  | populations                               | 25    |
|      | iterations                                | 100   |
|      | individual learning factor                | 2     |
|      | social learning factor                    | 2     |
|      | inertia factor                            | 0.8   |
|      | maximum speed                             | 0.8   |

ranging measurement, the coordinates of moving vehicle are calculated using QPSO in the i-BMQ localization algorithm. We also use multilateral localization(ML) and PSO to calculate the coordinates of moving vehicle as comparisons.

The parameters settings of QPSO and PSO are shown in Table III.

When the moving vehicle travels on the Campus every day, it can real time receive the signal surrounding base stations. Once the signals of more than 3 base stations are received simultaneously, the location of the moving vehicle is calculated using the proposed i-BMQ localization algorithm. The localization results are shown in Fig. 11.

As shown in Fig. 11, it can be observed clearly that the calculated coordinates using the i-BMQ localization algorithm are closer to the actual trajectory than the other localization algorithms. The better location performance benefits from the more accurate ranging results and the better capability to reach global optimum of the i-BMQ localization algorithm.

The localization errors of the i-BMQ localization algorithm and the other localization algorithms are shown in Fig. 12. The results indicate that the other localization algorithms have a bigger location errors and a larger fluctuation compared with the proposed i-BMQ localization algorithm. The localization error of the other localization algorithms is more than 40 meters. On the contrary, the localization error of the i-BMQ localization algorithm is relatively stable, and the localization error is lower than 40 meters. The analysis results show that the i-BMQ localization algorithm has a better location performance than the other localization algorithms.

The number of connected base stations simultaneously is a vital factor for the localization accuracy. The localization errors according to the different number of connected base stations are shown in Table IV.

As shown in Table IV, the proposed i-BMQ localization algorithm has higher localization accuracy than the other

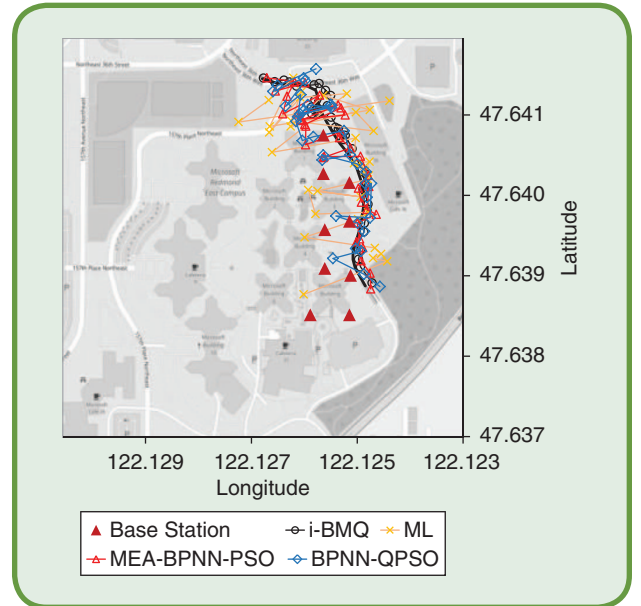


FIG 11 Localization results.

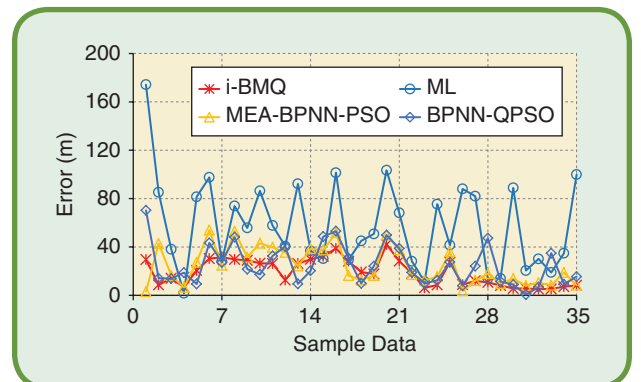


FIG 12 Localization errors.

Table IV. Mean localization error under the different number of connected base stations.

| Num. of connected base stations | i-BMQ (m) | MEA-BPNN-PSO (m) | BPNN-QPSO (m) | ML-LDM (m) |
|---------------------------------|-----------|------------------|---------------|------------|
| 4                               | 25.17     | 32.84            | 32.40         | 66.31      |
| 5                               | 22.69     | 25.95            | 25.44         | 60.01      |
| 6                               | 27.69     | 32.36            | 28.91         | 61.31      |
| 7                               | 17.95     | 25.70            | 19.99         | 58.46      |
| 8                               | 9.42      | 11.55            | 22.31         | 48.76      |
| 9                               | 6.44      | 11.07            | 12.43         | 43.84      |
| Average                         | 19.00     | 24.42            | 25.05         | 57.85      |

localization algorithms. The average localization accuracy is about 19 meters, and the best localization error is less than 10 meters. The localization accuracy shows an improving tendency with the increasing of the number of base stations connected to moving vehicle. This is consistent with our common sense that moving vehicle will achieve a more accurate location in dense base stations environments. The localization accuracy shows an exception when the six base stations is connected to the moving vehicle, which is caused by the less sample data. In other words, moving vehicle has a smaller chance to connect with six base stations simultaneously.

#### IV. Conclusions

The wireless localization is one of the most interesting research topics around connected vehicles. Both the improvement of path-loss model and the optimization of localization accuracy in wireless localization affect the positioning accuracy of moving vehicle. In this study, a novel double-layer architecture of wireless localization algorithm, integrating BPNN-MEA and quantum-behaved PSO algorithm, is proposed to improve the wireless positioning accuracy in field environment. BPNN-MEA is designed to establish a path-loss model among distance, RSSI value and travelling state of moving vehicle (location, speed and heading angle) to optimize the initial weights and thresholds, and QPSO algorithm is adopted to optimize the localization accuracy of moving vehicle in-field environment. The research results show that the path-loss model calibrated by BPNN-MEA in the i-BMQ localization algorithm has the lower error. Furthermore, the calculated coordinates by the i-BMQ localization algorithm are closer to the actual trajectory than the other localization algorithms, and has lower cumulative error and less oscillation, which indicates the proposed wireless localization algorithm has higher localization accuracy. The average localization error of the proposed i-BMQ localization algorithm is about 19 meters. Furthermore, when the number of base stations connected to the moving vehicle is larger than 7, the mean localization error

is less than 10 meters. For the wireless localization in field environment, this result is acceptable for CV applications.

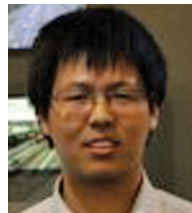
#### Acknowledgment

This work was financially supported by the National Natural Science Foundation of China (Grant no. 61473028), Beijing Municipal Natural Science Foundation (Grant no. 8162031), and the fundamental research funds for the central universities (Grant no. 2017JBM040).

#### About the Authors



**Lei Chen** received the B.E. degree in 2015 from Beijing Jiaotong University, Beijing, China. He is currently taking a successive postgraduate and doctoral program in the School of Traffic and Transportation, Beijing Jiaotong University, Beijing, China. His research interests include application technologies of connected vehicles, traffic big data analysis.



**Jiangfeng Wang** received the Bachelor degrees from the Department of Vehicle Operation Engineering in 2001 and received the Master degrees from Department of Traffic Information Engineering and Control in 2004, Jilin University, Changchun, China. He earned his Ph.D. degree in automobile engineering from Beihang University, Beijing, China, in 2007. He is currently working as a professor of the School of Traffic and Transportation, Beijing Jiaotong University, Beijing, China. His current research includes intelligent transportation system, traffic big data and active traffic safety.



**Zhijun Gao** received the B.E. degree in 2015 from Inner Mongolia University, Hohhot, China. He is currently working toward the Ph.D. degree in Beijing Jiaotong University, Beijing, China. His research interests include traffic flow theory, traffic behavior analysis and microcosmic traffic simulation under connected vehicle environment.



**Jiakuan Dong** received the B.S. degree in 2017 from Wuhan University of Technology, Wuhan, China. He is currently working toward the master's degree with the School of Traffic and Transportation, Beijing Jiaotong University, Beijing, China. His research interests include traffic data mining and driving behavior research under connected vehicles environment.



**Xuedong Yan** served as a post-doctoral researcher in University of Florida during 2005 and 2007. He has been the scientific research director of South-eastern Transportation Center from 2007 to 2011. He is currently working as a professor of the School of Traffic and Transportation, Beijing Jiaotong University, Beijing, China. His current research includes city planning, traffic planning, traffic safety, driving simulator application and traffic data statistics and model analysis.



**Jian Wang** received his Bachelor and Master degrees from Jilin University of Technology in 1995 and 1998 respectively. He earned his Ph.D. degree in the institute of mechanical science and engineering from Jilin University, Changchun, China, in 2001. He is currently working as an associate professor of the School of Transportation Science and Engineering, Beihang University, Beijing, China. His current research includes intelligent transportation system and traffic safety.

## References

- [1] N. J. Goodall, B. L. Smith, and B. Park, "Microscopic estimation of freeway vehicle positions from the behavior of connected vehicles," *J. Intell. Transport. Syst.*, vol. 20, no. 1, pp. 45–54, 2016.
- [2] X. T. Duan, Y. P. Wang, D. X. Tian, "A vehicular positioning enhancement with connected vehicle assistance," in *Proc. IEEE 82nd Vehicular Technology Conf.*, Boston, USA, 6–9 Sept. 2015, pp. 1–8.
- [3] N. J. Goodall, B. Park, and B. L. Smith, "Microscopic estimation of arterial vehicle positions in a low-penetration-rate connected vehicle environment," *J. Transport. Eng.*, vol. 140, no. 10, pp. 1–10, 2014.
- [4] J. Q. Wang, D. H. Ni, and K. Q. Li, "RFID-based vehicle positioning and its applications in connected vehicles," *Sensors*, vol. 14, no. 3, pp. 4225–4238, 2014.
- [5] M. Borenovic, A. Neskovic, and N. Neskovic, "Vehicle positioning using GSM and cascade-connected ANN structures," *IEEE Trans. Intell. Transp. Syst.*, vol. 14, no. 1, pp. 34–46, 2013.
- [6] F. Heng, "The design of the vehicle location system based on wireless sensor network," in *Proc. Int. Industrial Informatics and Computer Engineering Conf.*, Xi'an, China, 10–11 Jan. 2015, pp. 558–541.
- [7] K. Yang, Y. Z. Zhu, Q. Yang, "Design of wireless positioning system based on technology of communication between vehicle-to-vehicle," in *Proc. Int. Industrial Informatics and Computer Engineering Conf.*, Xi'an, China, 10–11 Jan. 2015, pp. 1803–1806.
- [8] Q. J. Deng, D. Czarkowski, M. Bojarski, "Edge position detection of on-line vehicles with segmental wireless power supply," in *Proc. IEEE Int. Electric Vehicle Conf.*, Florence, Italy, 17–19 Dec. 2014, pp. 1–8.
- [9] S. Rezaei, R. Sengupta, and H. Krishnan, "Tracking the position of neighboring vehicles using wireless communications," *Transport. Res. Part C, Emerg. Technol.*, vol. 18, no. 3, pp. 335–350, 2010.
- [10] J. F. Wang, F. Gao, F. Yi, "Design of wireless positioning algorithm of intelligent vehicle based on VANET," in *Proc. IEEE Intelligent Vehicles Symp.*, Xi'an, China, 3–5 Jan. 2009, pp. 1098–1102.
- [11] A. Gil-Pinto, P. Fraisse, R. Zapata, "Wireless reception signal strength for relative positioning in a vehicle robot formation," in *Proc. IEEE Latin American Robotics Symp.*, Santiago, Chile, 26–27 Oct. 2006, pp. 112–118.
- [12] L. S. Guo and Q. Zhang, "Wireless data fusion system for agricultural vehicle positioning," *Biosyst. Eng.*, vol. 91, no. 3, pp. 261–269, 2005.
- [13] Y. B. Yao, Q. Han, X. R. Xu, and N. L. Jiang, "A RSSI-based distributed weighted search localization algorithm for WSNs," *Int. J. Distrib. Sens. Netw.*, vol. 11, no. 4, pp. 1–11, 2015.
- [14] N. Alam, A. T. Balaie, and A. G. Dempster, "A DSRC doppler-based cooperative positioning enhancement for vehicular networks with GPS availability," *IEEE Trans. Veh. Technol.*, vol. 60, no. 9, pp. 4462–4470, 2011.
- [15] X. Song, X. Li, W. Tang, W. Zhang, and B. Li, "A hybrid positioning strategy for vehicles in a tunnel based on RFID and in-vehicle sensors," *Sensors*, vol. 14, no. 12, pp. 23095–23118, 2014.
- [16] J. Graefenstein, M. E. Bouzouraa, "Robust method for outdoor localization of a mobile robot using received signal strength in low power wireless networks," in *Proc. IEEE Int. Conf. Robotics and Automation*, Pasadena, USA, 19–25 May 2008, pp. 33–38.
- [17] S. K. Gharghan, R. Nordin, M. Ismail, and J. A. Ali, "Accurate wireless sensor localization technique based on hybrid PSO-ANN algorithm for indoor and outdoor track cycling," *IEEE Sens. J.*, vol. 16, 2, pp. 529–541, 2016.
- [18] Y. Sung, "RSSI-based distance estimation framework using a Kalman filter for sustainable indoor computing environments," *Sustainability*, vol. 8, no. 11, p. 1156, 2016.
- [19] W. A. Zhang, X. Yang, L. Yu, and S. Liu, "Sequential fusion estimation for RSS-based mobile robots localization with event-driven WSNs," *IEEE Trans. Ind. Inform.*, vol. 12, no. 4, pp. 1519–1528, 2016.
- [20] M. Kadkhoda, A. T. Mohammad-R, M. H. Yaghmaee, Z. Davarzani, "A probabilistic fuzzy approach for sensor location estimation in wireless sensor networks," in *Proc. IEEE Int. Conf. Fuzzy Systems*, Barcelona, Spain, 18–25 July 2010, pp. 1–11.
- [21] J. Zou, S. Gundry, J. Kusyk, C. S. Sahin, "Particle swarm optimization based topology control mechanism for holonomic unmanned vehicles operating in three-dimensional space," in *Proc. IEEE Sarnoff Symp.*, Newark, USA, 21–22 May 2012, pp. 1–5.
- [22] Y. Wang, X. Ma, M. Xu, Y. Liu, and Y. Wang, "Two-echelon logistics distribution region partitioning problem based on a hybrid particle swarm optimization-genetic algorithm," *Expert Syst. Appl.*, vol. 42, no. 12, pp. 5019–5031, 2015.
- [23] M. Yusoff, J. Ariffin, A. Mohamed, "A multi-valued discrete particle swarm optimization for the evacuation vehicle routing problem," in *Proc. Int. Conf. Advances Swarm Intelligence*, Chongqing, China, 12–15 June 2011, pp. 182–193.
- [24] D. Li and X. B. Wen, "An improved PSO algorithm for distributed localization in wireless sensor networks," *Int. J. Distrib. Sens. Netw.*, vol. 8, pp. 184–189, 2015.
- [25] M. Okulewicz, J. Mandziuk, "Two-phase multi-swarm PSO and the dynamic vehicle routing problem," in *Proc. IEEE Symp. Computational Intelligence for Human-like Intelligence*, Orlando, USA, 9–12 Dec. 2014, pp. 1–8.
- [26] E. B. Anitha and K. S. Duraiswamy, "A new hybrid approach for prediction of moving vehicle location using particle swarm optimization and neural network," *J. Theor. Appl. Inf. Technol.*, vol. 59, no. 3, pp. 791–800, 2014.
- [27] Q. Ni, "An improved node localization method for wireless sensor network based on PSO and evaluation of environment variables," *Adv. Swarm Intell.*, vol. 9713, pp. 324–332, 2016.
- [28] B. Jack, "Improving indoor positioning accuracy with dense, cooperating beacons," *Procedia Comput. Sci.*, vol. 40, pp. 1–8, 2014.
- [29] C. Matteo, L. Frédéric, C. Philippe, S. François, "Wi-Fi-based indoor positioning: basic techniques, hybrid algorithms and open software platform," in *Proc. Int. Conf. Indoor Positioning and Indoor Navigation*, Zürich, Switzerland, 15–17 Sept. 2010, pp. 1–10.
- [30] K. R. Anne, K. Kyamakya, F. Erbas, C. Takenga, J. C. Chedjou, "GSM RSSI-based positioning using extended Kalman filter for training artificial neural networks," in *Proc. Vehicular Technology Conf.*, Los Angeles, USA, 26–29 Sept. 2004, pp. 4141–4145.
- [31] A. Awad, T. Frunzke, F. Dressler, "Adaptive distance estimation and localization in WSN using RSSI measures," in *Proc. 10th Euromicro Conf. Digital System Design Architectures, Methods Tools (DSD)*, 2007, pp. 471–478.
- [32] K. S. Low, H. A. Nguyen, H. Guo, "A particle swarm optimization approach for the localization of a wireless sensor network," in *Proc. IEEE Int. Symp. Industrial Electronics*, 2008, pp. 1820–1825.
- [33] D. Li, "Wireless sensor network based on genetic algorithm of localization algorithms," *Comput. Simul.*, vol. 9, pp. 161–164, 2011.
- [34] R. Mahajan, J. Zahorjan, B. Zill, "Understanding WIFI-based connectivity from moving vehicles," in *Proc. IMC 07: ACM SIGCOMM Conf. Internet Measurement*, San Diego, CA, USA, 26 Oct. 2007, pp. 321–32625.
- [35] A. S. Hassan, S. H. Bouk, A. Mehmood, N. Javaid, S. Iwao, "Effect of fast moving object on RSSI in WSN: an experimental approach," in *Proc. Int. Multi Topic Conf.*, Berlin, Heidelberg: Springer, 2012, vol. 281, pp. 43–51.
- [36] R. Miucic, Z. Popovic, S. M. Mahmud, "Experimental characterization of DSRC signal strength drops," in *Proc. Int. IEEE Conf. Intelligent Transportation Systems*, 2009, pp. 1–5.
- [37] X. Wan, Z. Zheng, and G. C. Wan, "An RSSI-based differential correlation algorithm for wireless node localization," *Open Autom. Control Syst. J.*, vol. 5, no. 1, pp. 73–79, 2013.